New Trends in Nuclear Physics Detectors 2021

Nuclear Astrophysics Experiments using Active Target Detectors at CENS

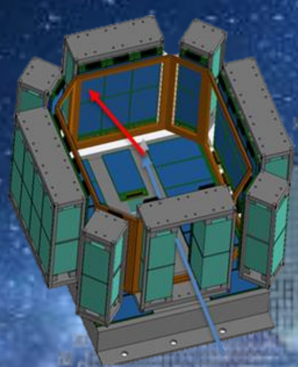

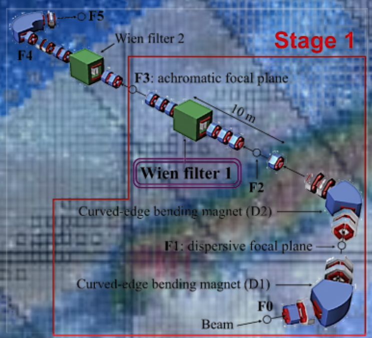

Sunghoon(Tony) Ahn

CENS, IBS

October 25th, 2021

On be half of TexAT & AToM-X collaborations

Institute for Basic Science

New Trends in Nuclear Physics Detectors 2021

Nuclear Astrophysics Experiments using Active Target Detectors at CENS

1. Center for Exotic Nuclear Studies (CENS)
2. Nuclosynthesis and Nuclear Physics Inputs
3. $^{14}O(\alpha,p)^{17}F$ cross sections using TexAT
4. AToM-X Development at CENS
5. Future Experimental Studies
6. Summary

CENS Organization

SINCE 2019

Kevin Insik Hahn

CENS Director

Advisory Committee

https://www.ibs.re.kr/cens/

Nuclear Astrophysics

Group Leader

- Nucleosynthesis
- r−process, rp−process nuclei
- Collaboration and utilization of KoBRA
- Nuclear Spectroscopy

Nuclear Structure

Group Leader

- Sh
- St isc
- Cl
- Ne As

Nuclear Reaction

Group Leader

Nuclear Theory

Group Leader

- Reaction Calculations
- Low Energy Nuclear Physics
- Nuclear Structure Models
- QRPA & DQRPA Models

4 group leaders
3 senior researchers
9 postdocs
6 students
2 secretaries

CENS Objectives

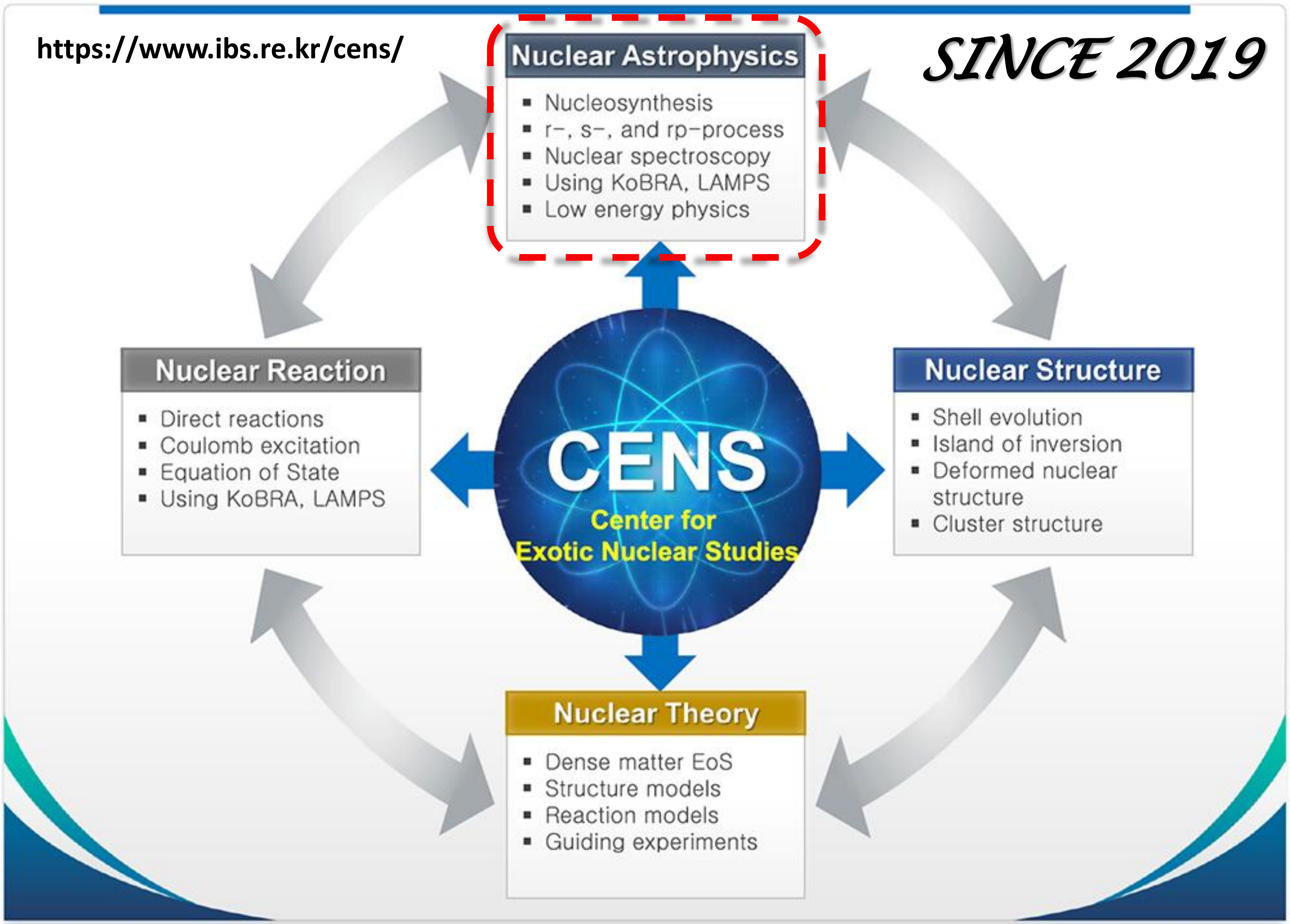

CENS Nationalities and Playgrounds

Nationalities	RIB Facilities
Canada	RIBF (Japan)
Hungary	CRIB/CNS (Japan)
South Korea	ATOMKI (Hungary)
Turkey	HI-ISOLDE (Switzerland)
USA	GANIL (France)
China	TRIUMF (Canada)
Spain	TAMU (USA)
	FRIB (USA)
	ANL (USA)
	RAON (South Korea)

Abundance Pattern of Elements

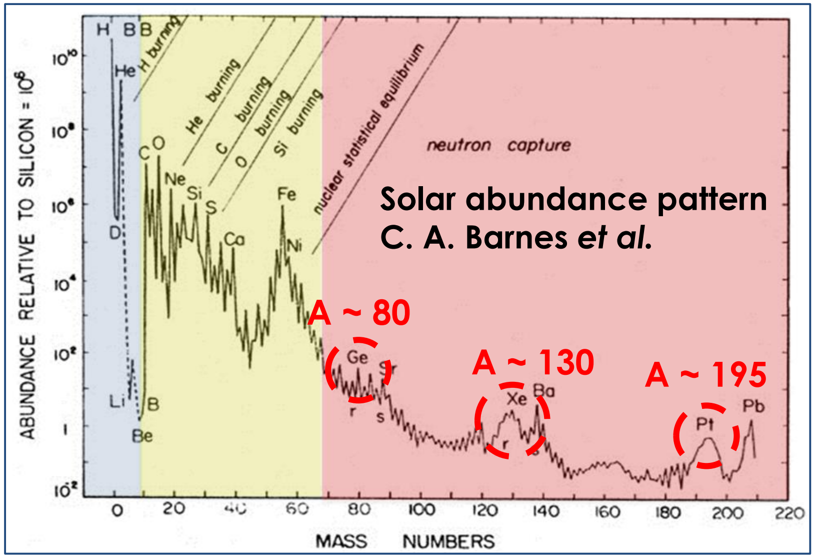

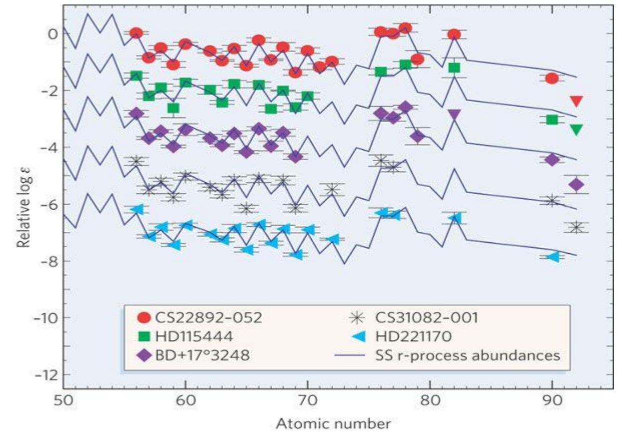

Abundances in metal poor r-stars
J.J. Cowan and C. Sneden, *Nature* 440, 1151 (2006)

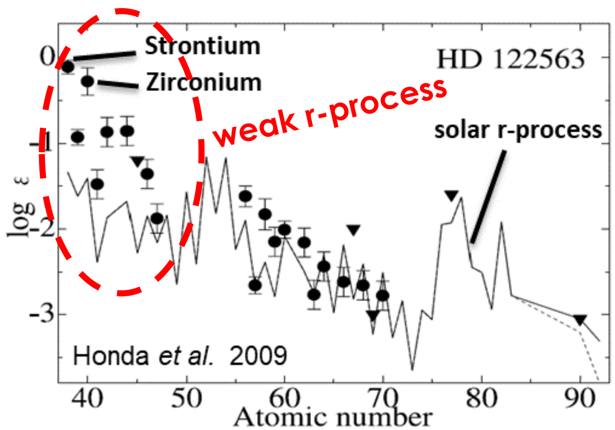

Abundance pattern of a Metal Poor Halo Star

Falk Herwig *et al.* 2014

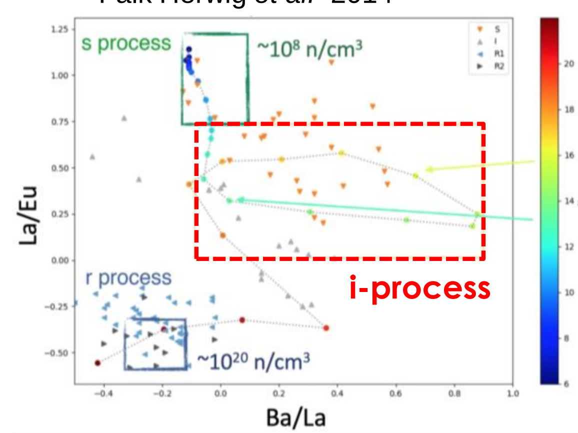

Abundance ratio of La/Eu and Ba/La

Nucleosynthesis Processes

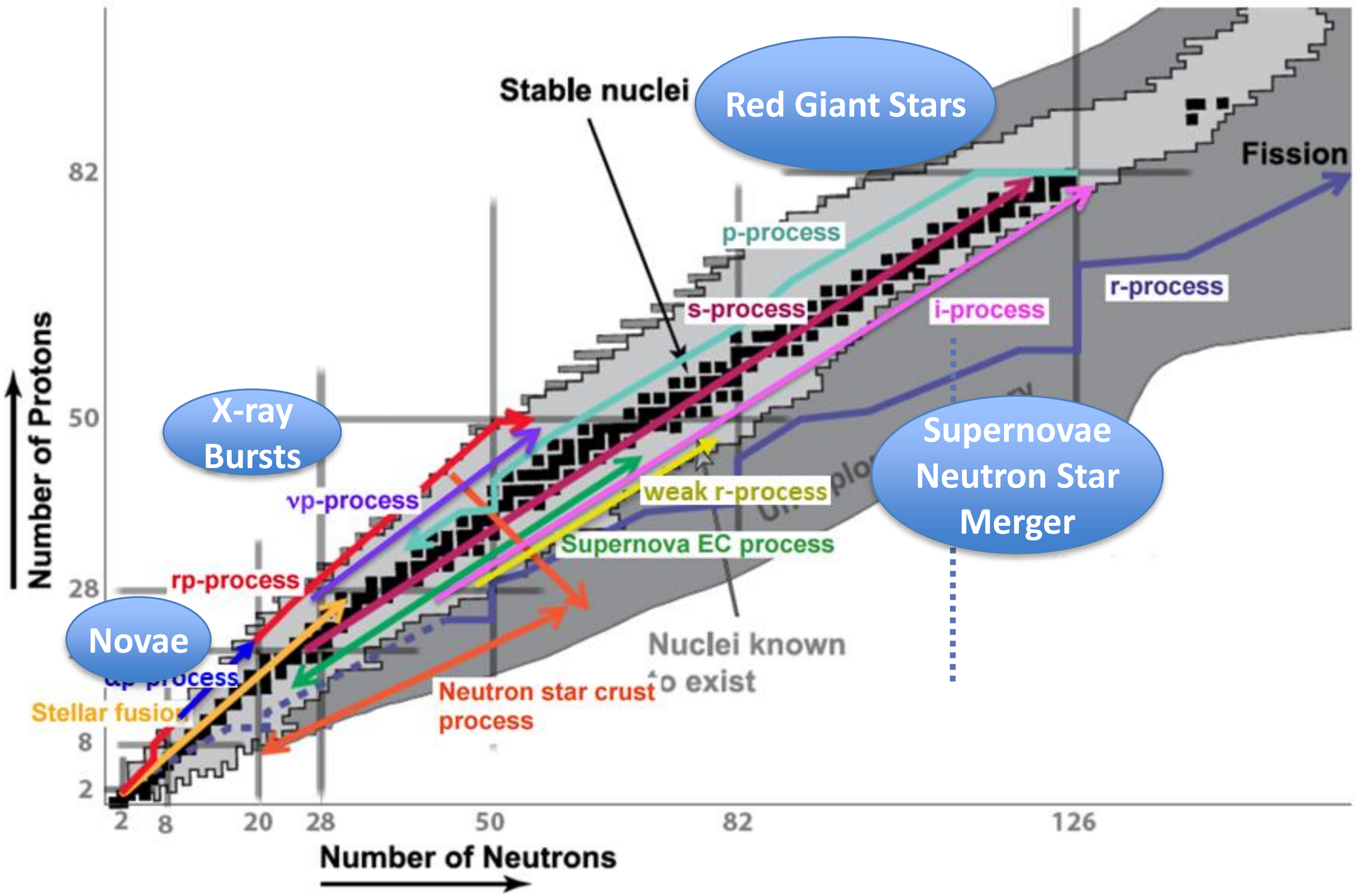

Schematic overview of the nuclear processes on nuclear chart
H. Schatz, 2016

Nuclear Properties for Nucleosynthesis

- Nucleosynthesis process can explain the observation.
  → **Nuclear Physics plays an important role!**
  → **mass**, Q-value, $\mathbf{T_{1/2}}$, $\mathbf{P_n}$, level densities and **reaction rates**

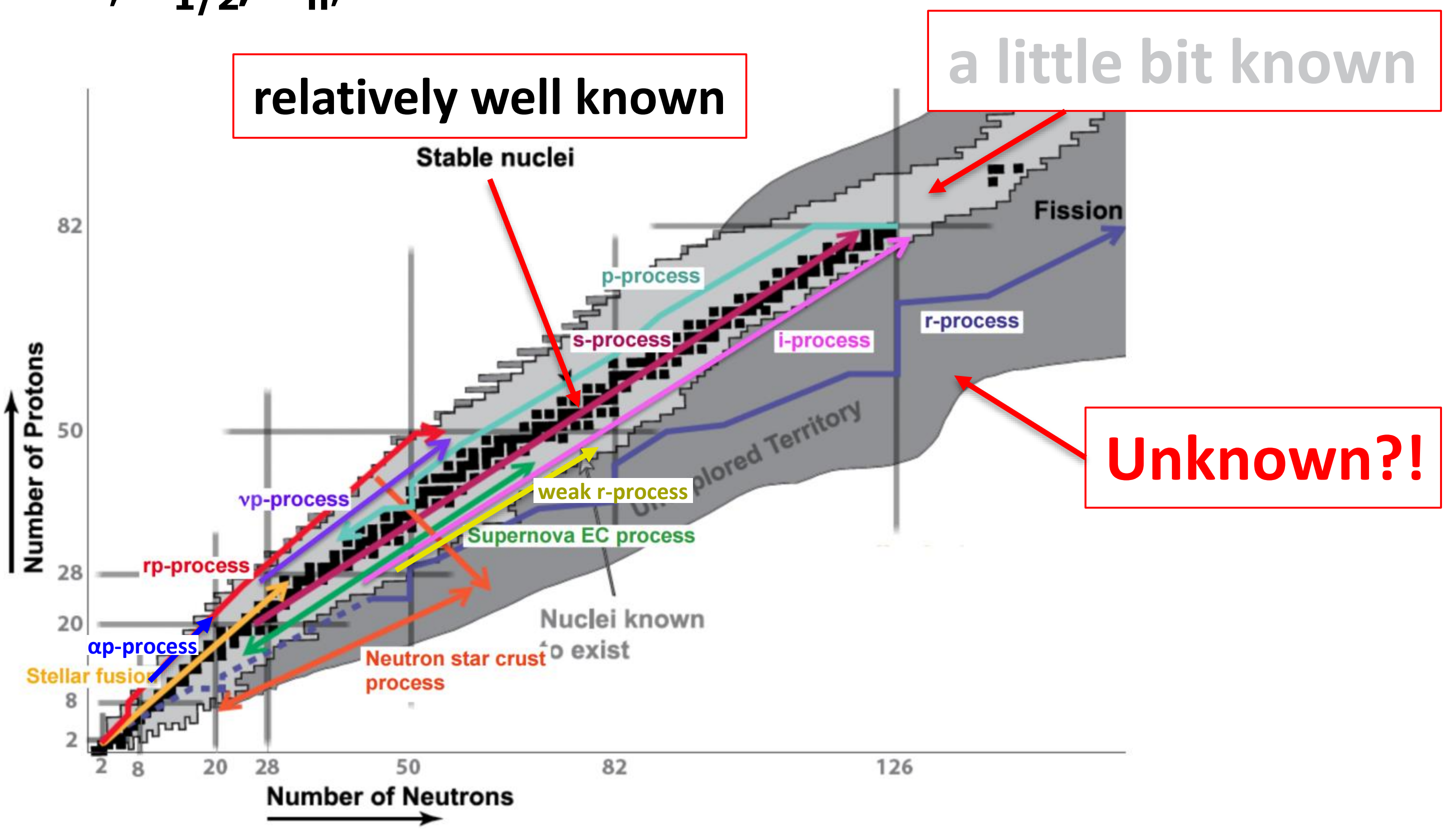

Schematic overview of the nuclear processes on nuclear chart
H. Schatz, 2016

Nuclear Reaction Rates during the αp-process

- Light curves of x-ray burst can be explained by αp-process and rp-process.
- (α,*p*) reaction rates play an important role in determining the light curve.

J.J.M. in 't Zand *et al.* 2017

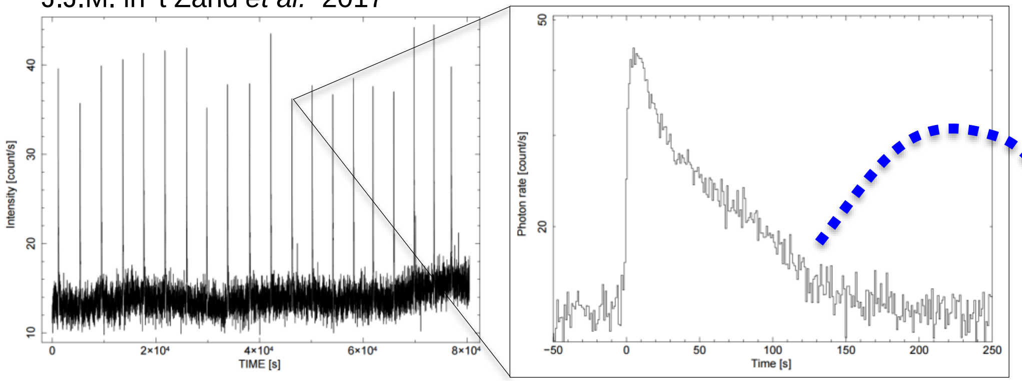

Observed light curves of X-ray burst

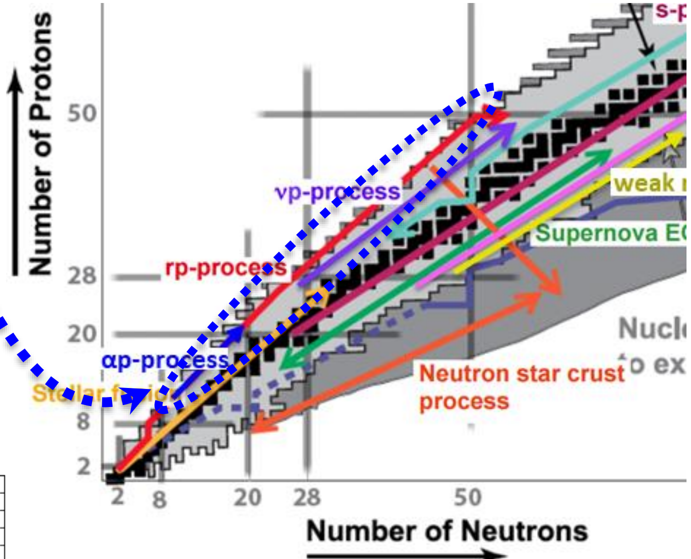

R. H. Cyburt *et al.* 2016

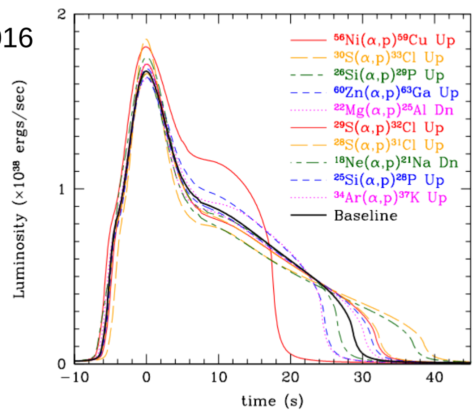

Calculated light curves of X-ray burst

The most important (α,p) cross sections in X-ray burst

- The recent sensitivity study shows there are important astrophysical (*α,p*) reaction rates affecting a large variation of energy generation and final ash in X-ray burst model.
- Possible Reactions with CRIB beams: ^{30}S(α,p)^{33}Cl, ^{26}Si(α,p)^{29}P, ^{22}Mg(α,p)^{25}Al, ^{18}Ne(α,p)^{21}Na, ^{14}O(α,p)^{17}F and ^{17}F(α,p)^{20}Ne

Rank	Reaction	Type	Sensitivity
1	^{15}O(α,γ)^{19}Ne	D	16
2	^{56}Ni(α,p)^{59}Cu	U	6.4
3	^{59}Cu(p,γ)^{60}Zn	D	5.1
4	^{61}Ga(p,γ)^{62}Ge	D	3.7
5	^{22}Mg(α,p)^{25}Al	D	2.3
6	**^{14}O(α,p)^{17}F**	D	5.8
7	^{23}Al(p,γ)^{24}Si	D	4.6
8	^{18}Ne(α,p)^{21}Na	U	1.8
9	^{63}Ga(p,γ)^{64}Ge	D	1.4
10	^{19}F(p,α)^{16}O	U	1.3

Reactions that Impact the Burst Light Curve in the Multi-zone X-ray Burst Mode

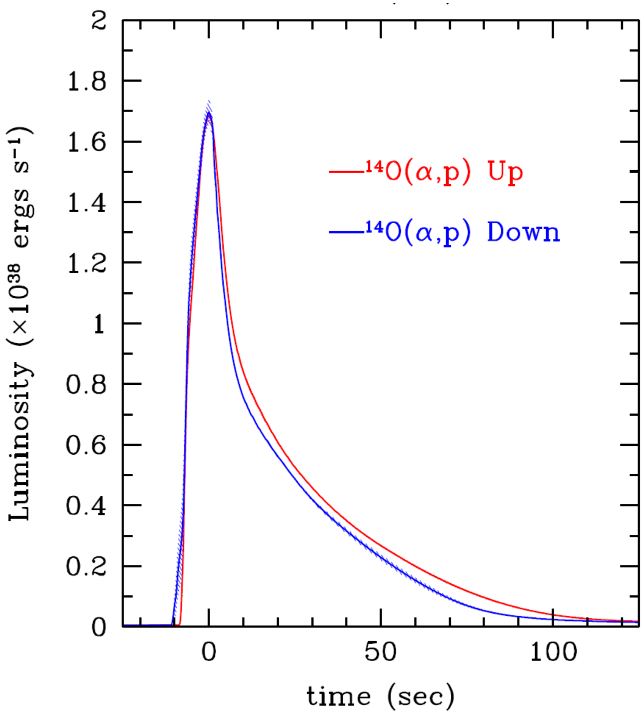

The X-ray burst light curve in the multi-zone varied by ^{14}O(α,p) reaction rate

Alternate break-out path from HCNO cycle

- Alternate path from the hot CNO cycle to the rapid proton burning (rp-process)
- Wallace and Woosley have shown that at sufficiently high temperatures and densities α capture on ^{14}O and ^{15}O competes favorably with β decay

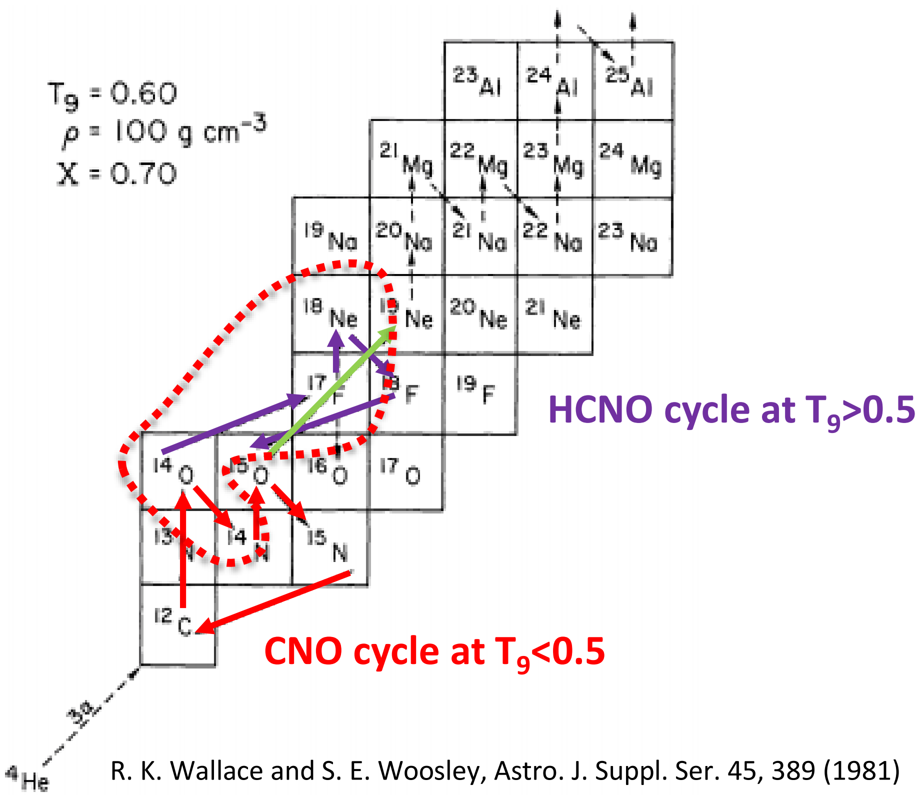

R. K. Wallace and S. E. Woosley, Astro. J. Suppl. Ser. 45, 389 (1981)

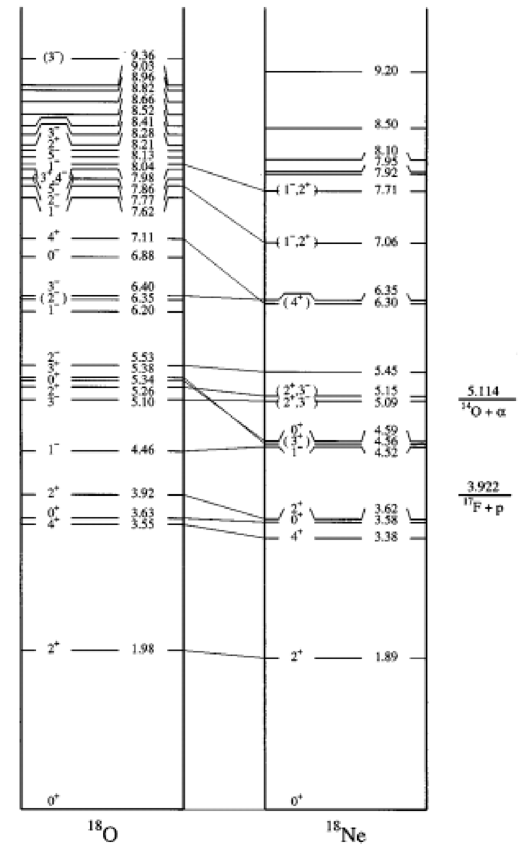

Experimental studies of $^{14}O(\alpha,p)^{17}F$ cross sections

- AZURE and TALYS-1.95 calculated cross sections: two orders of magnitude different.
- Previous cross section measurements studied at high energy range (2 MeV ≤ Ecm ≤ 2.8 MeV) show large disagreements with the measurement containing data at low energy range (1 MeV ≤ Ecm ≤ 1.5 MeV) encouraging another study to confirm the reliability of measurements.

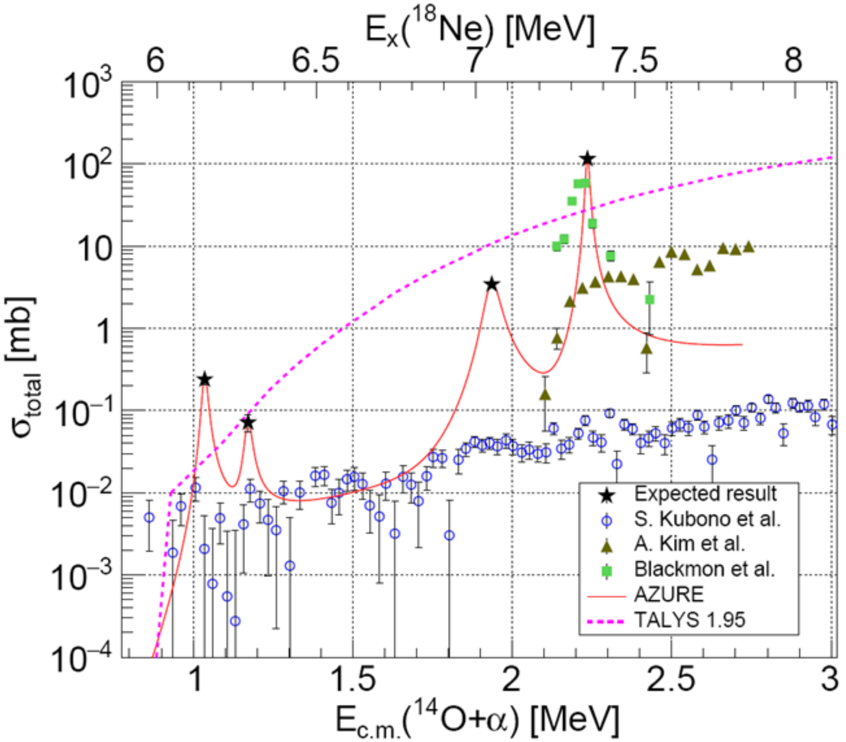

Previous measured data and calculated total cross sections of 14O(α,p) reaction

RIB Beam Production – CRIB/CNS at RIKEN

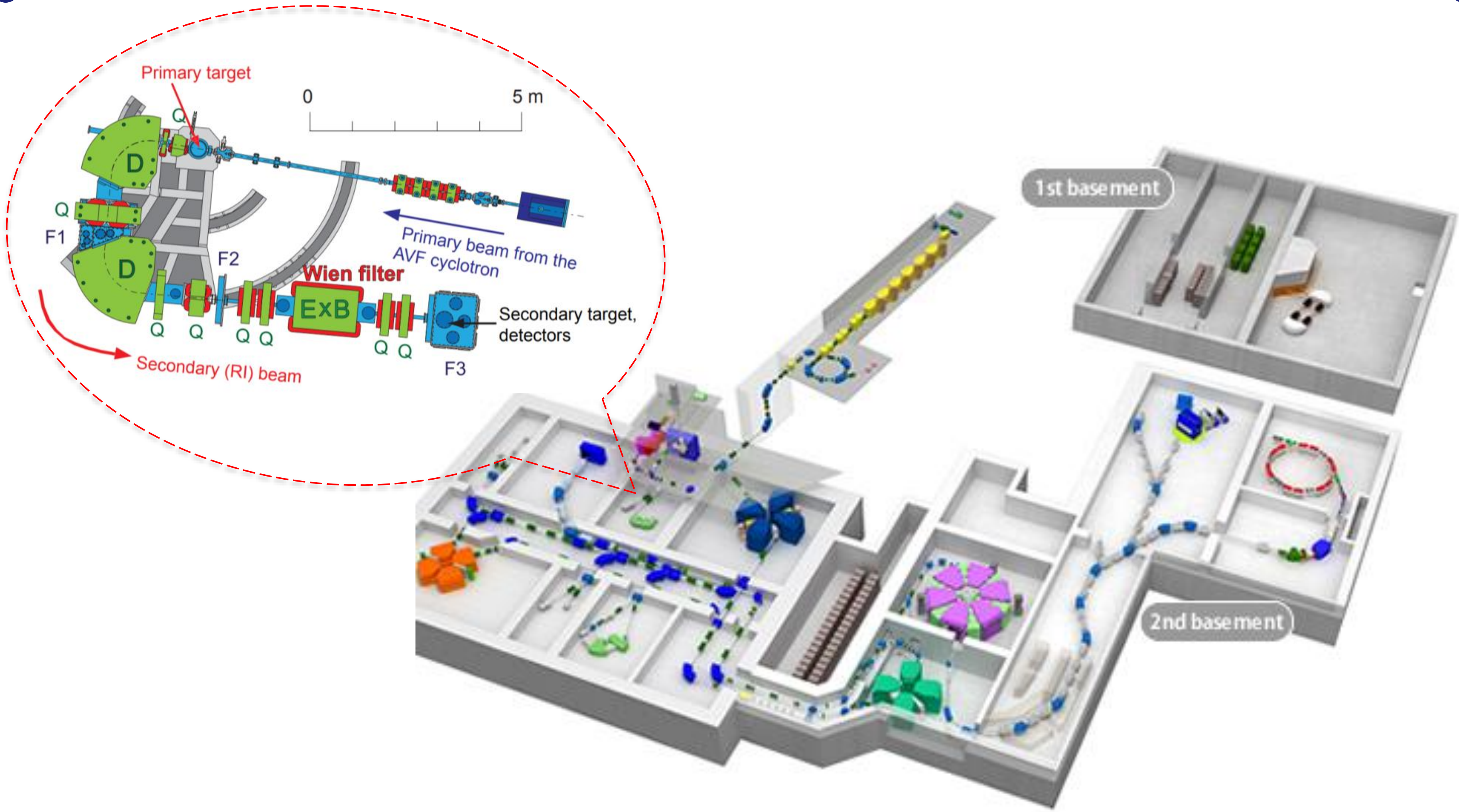

Radioactive beam by CNS RI beam separator (CRIB) at RIKEN Nishina Center

RIB Beam Production – CRIB/CNS at RIKEN

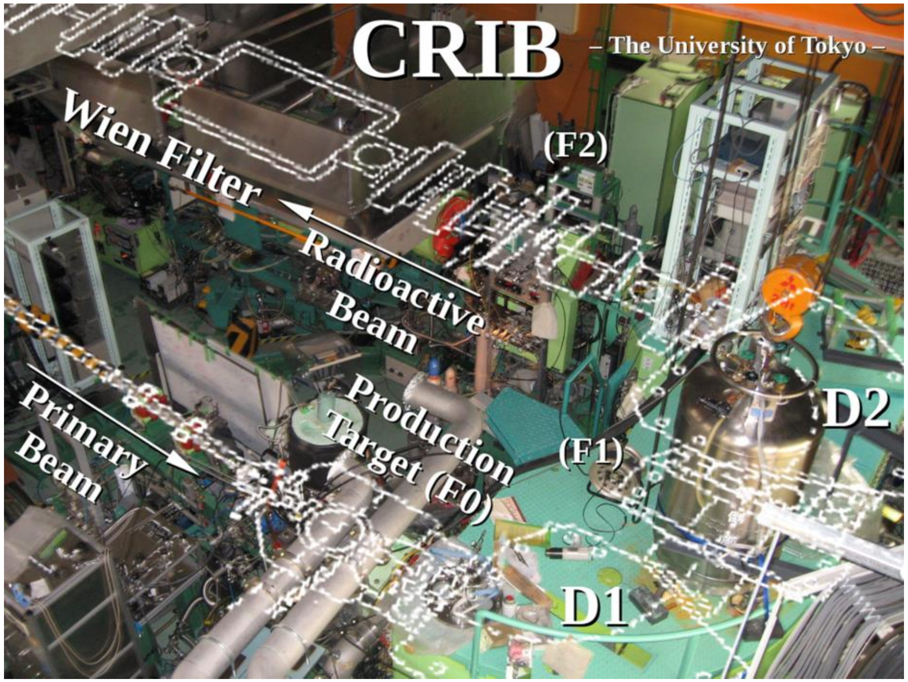

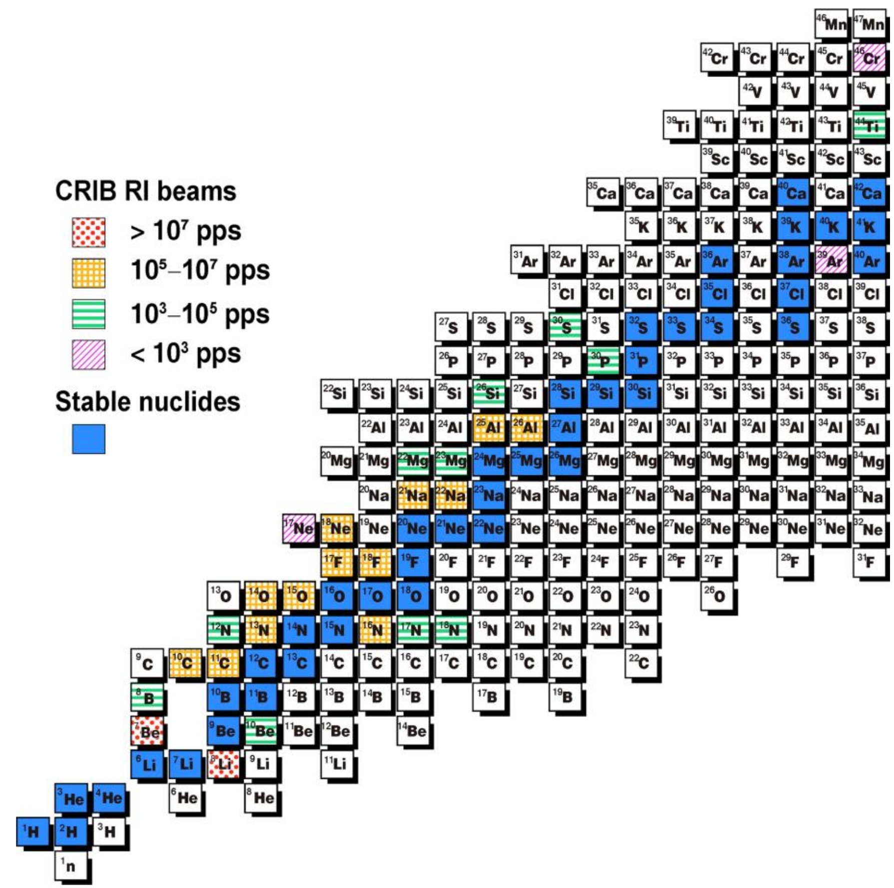

Radioactive beam by CNS RI beam separator (CRIB) at RIKEN Nishina Center

^{14}O beam production at CRIB

Primary beam	Energy	Intensity (pps)	Production target
^{14}N	8.4 MeV/u	1.00E+06	^{2}H, 90K, 230 Torr 1.29 mg/cm^2

Secondary beam	Energy	Intensity (pps)	Scattering target
^{14}O	3.36 MeV/u	3.00E+05	He+CO_2 (90%+10%) 460 Torr

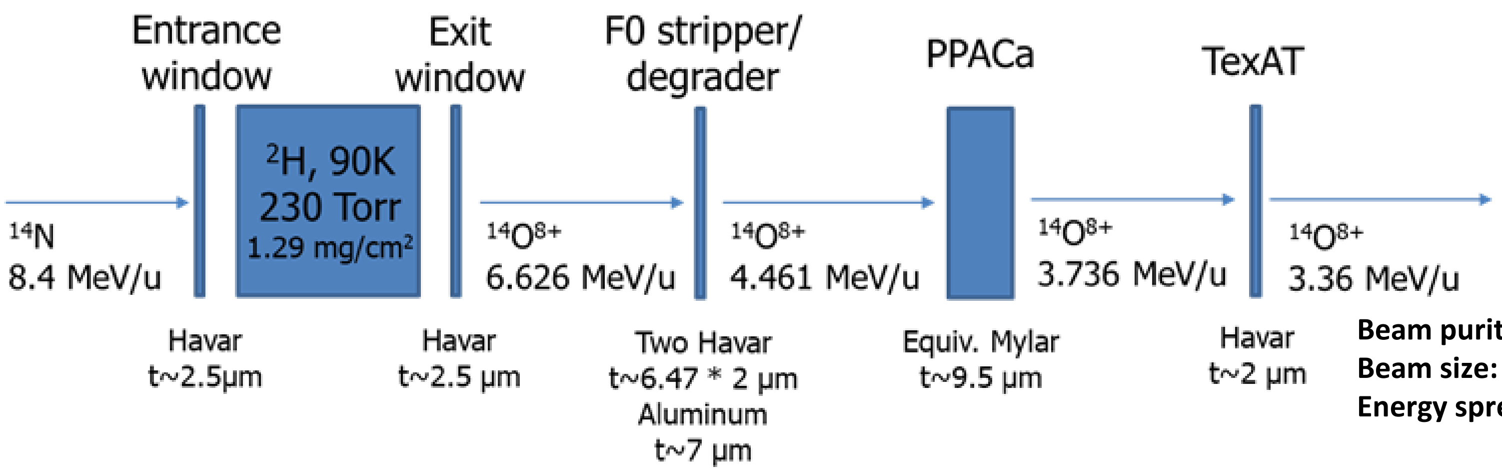

Beam purity: 90%
Beam size: 10mmD
Energy spread: 3%

A schematic diagram of the ^{14}O beam production from the CRIB/CNS

Texas Active Target Time Projection Chamber

- Active area: 245 (X) x 150 (Y) x 224 (Z) mm^3
- Scattering chamber: 500 (X) x 340 (Y) x 500 (Z) mm^3 (made of 3cm-thick aluminum) - portable!
- Ionization Counter after the window for beam intensity and purity
- Silicon and CsI detectors wall for total energy of particles
- Different front windows for physics needs (Havar, Mylar, Kapton and Ti)
- Target gas: CH_4, C_4H_{10}, CD_4, He/CO_2(98/2%) and CO_2

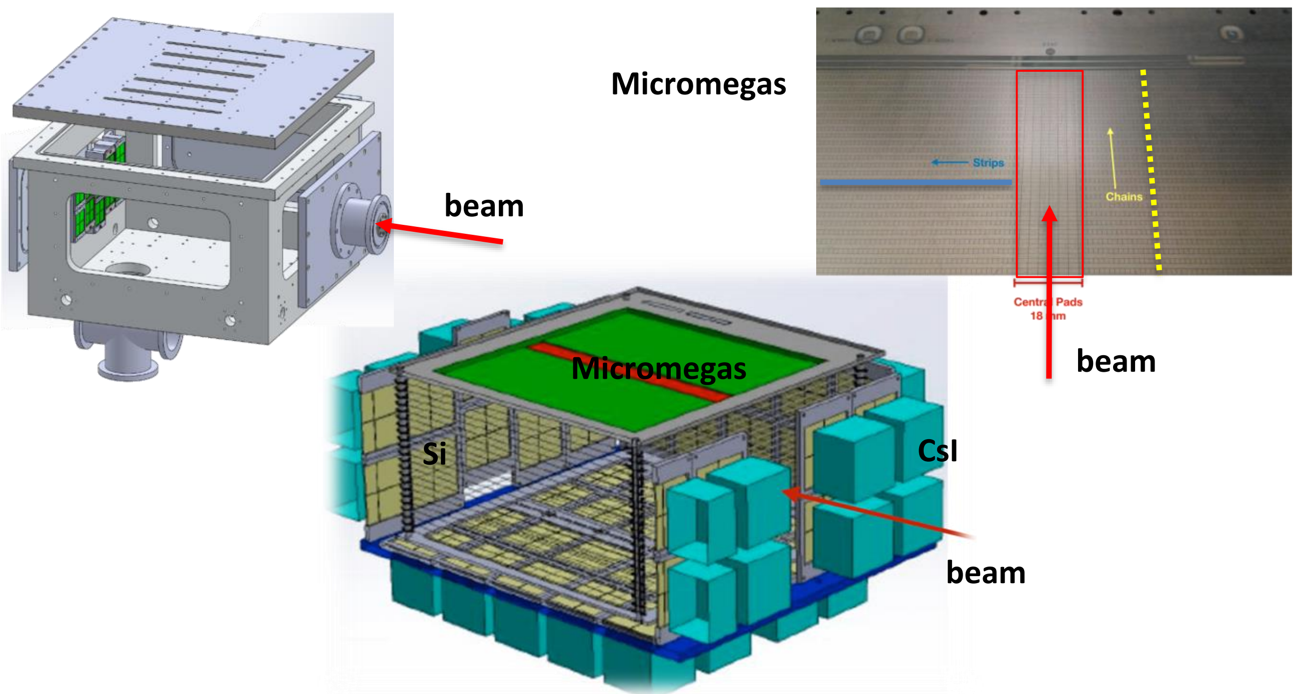

Texas Active Target (TexAT) design


A picture for TexAT and GET setup

Previous TexAT Experiment with RI Beam

- Reaction: $^{8}B + p$ with 7.6 MeV/u ^{8}B beam and 10^3 pps from MARS, Texas A&M University
- Target: Methane gas (CH_4), Pressure = 435 Torr
- The new $5/2^{+}$ state found at 4.3 MeV in ^{9}C

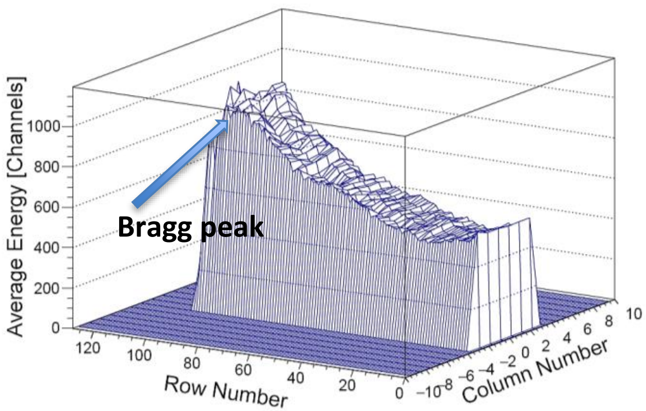

The energy deposition of ^{8}B in each pads.

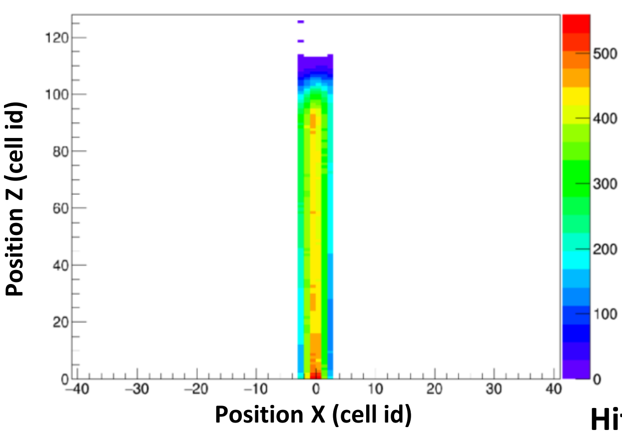

Hit pattern in the Micromegas Plate

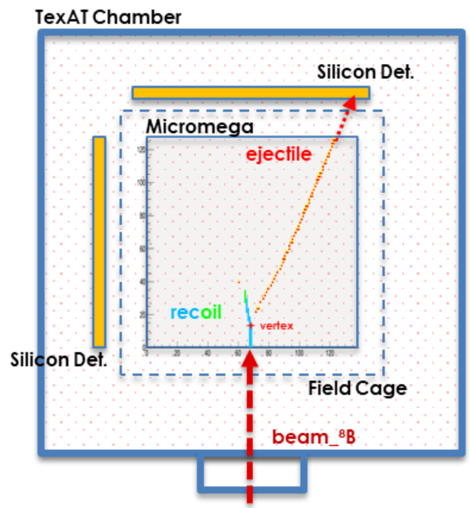

A sample particle track from ^{8}B+*p* experiment

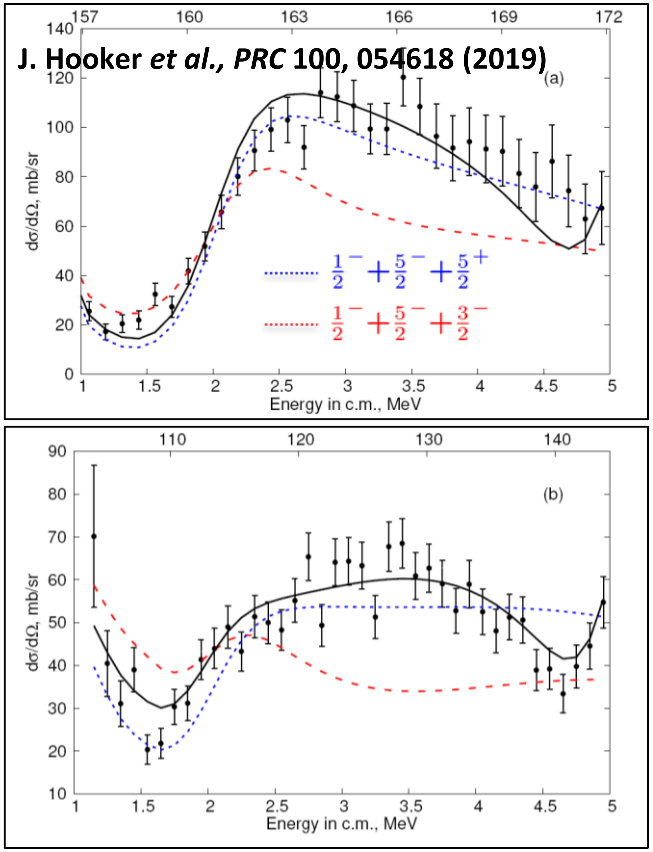

Excitation function for ^{8}B + p
(a) 157 - 172 deg.
(b) 100 – 145 deg. in CoM.

Direct Measurement of $^{14}O(\alpha,p)^{17}F$ cross sections with TexAT at CRIB

- Reaction: $^{14}O + \alpha$ with 3.36 MeV/u ^{14}O beam and 3×10^5 pps from CRIB
- Target: He/CO_2 (90/10 %) mixture gas, Pressure = 460 Torr (Beam will stop at Z=196 mm)
- Si + CsI detectors will be installed on the side and bottom of the field cage.
- Detector Efficiency from GEANT4 simulation: 50% (Si. Det Hit trigger, uniform cross section assumed)

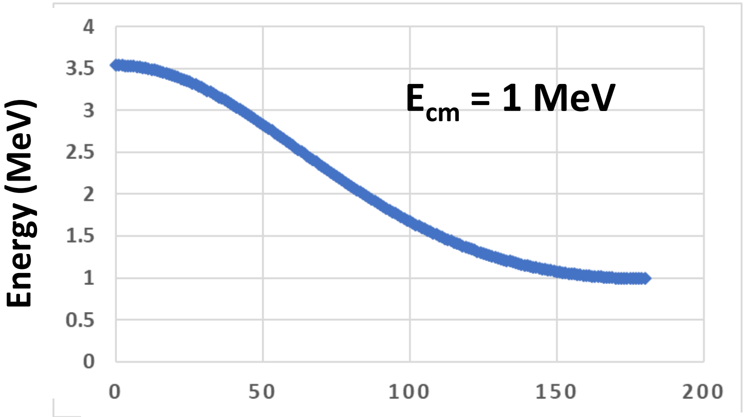

$^{14}O(\alpha,p)^{17}F$ reaction in inverse kinematics

Ep (MeV)	E_{remain} (MeV)
2.5	2.2
2	1.6
1.5	1
1	0.14

Proton Energy at Si detector for event at Z=168mm (E_{cm} = 1 MeV)

TexAT Chamber

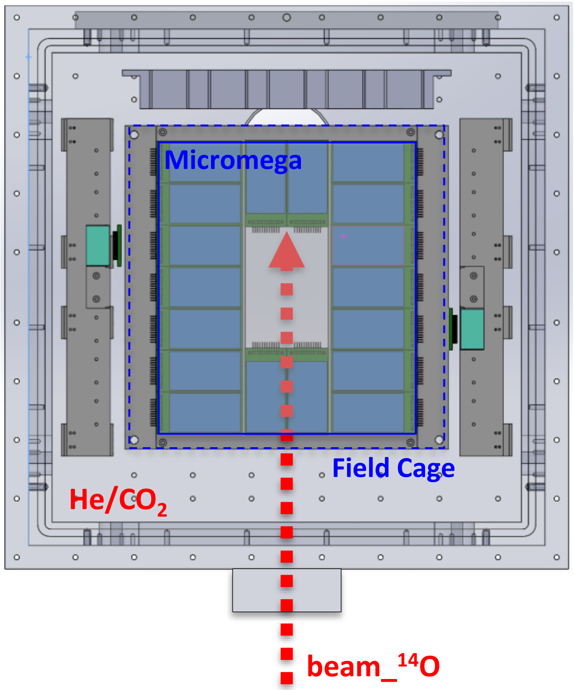

TexAT detector setup

TexAT Upgrade for $^{14}O(\alpha,p)^{17}F$ experiment

- FC Upgrade and Test

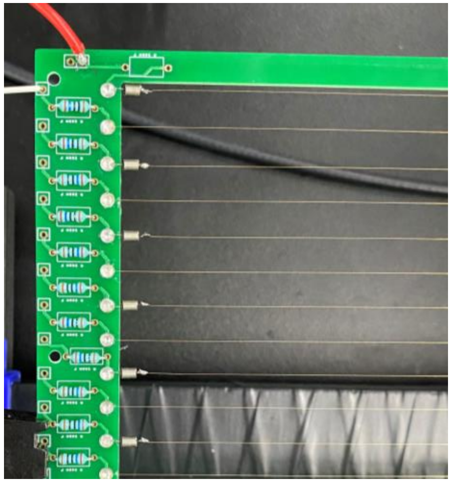

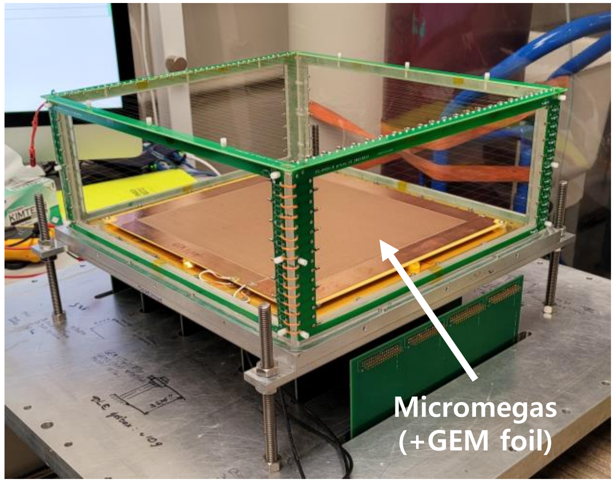

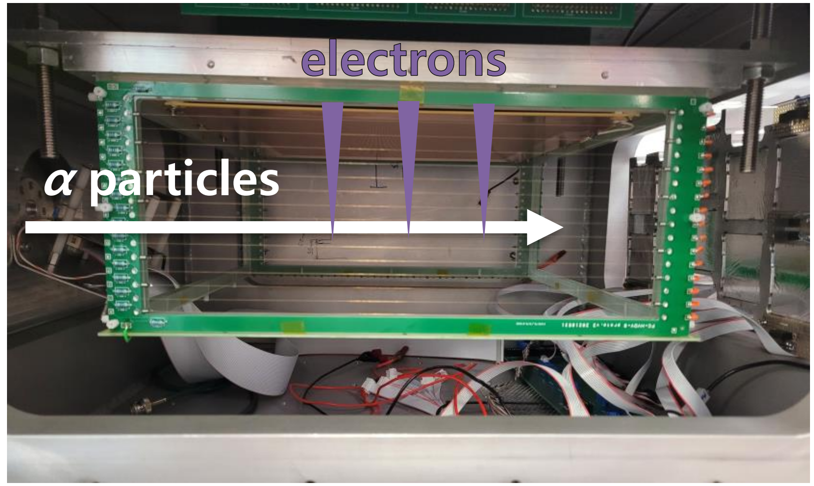

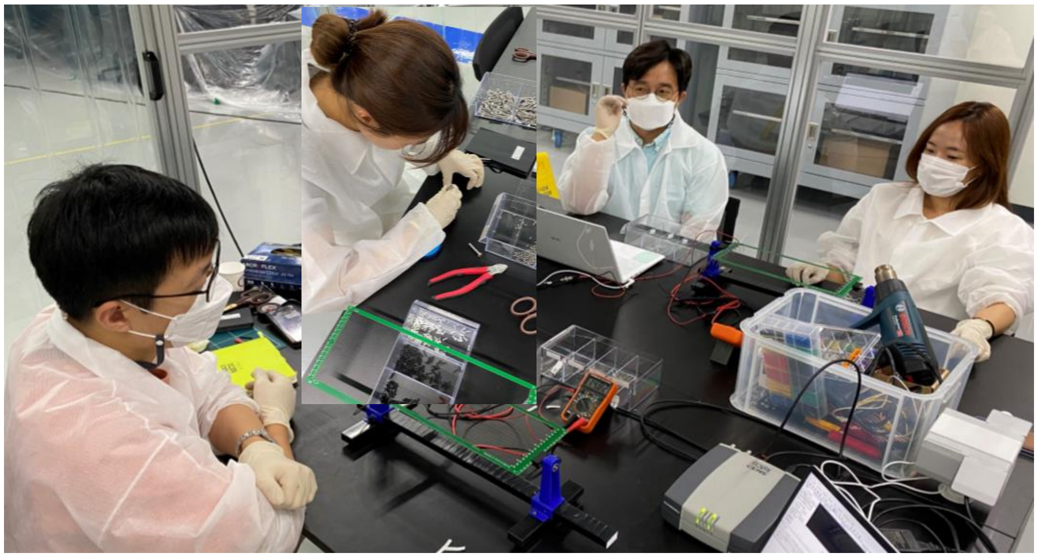

- using α-emitting ^{241}Am fission source
- α particle track could be obtained by the Micromegas
- checked edge effect
- compared with original TexAT field cage

Requested Experiment Beamtime

- Beam Time Request: 14 days total with beam intensity of 3 x 10^5 pps
  - ✓ TexAT optimization time with the stable ^{14}N primary beam: 0.5 day
  - ✓ beam tuning: 0.5 day
  - ✓ background runs with the CO_2 gas: 2 days
  - ✓ production runs with ^{14}O beam and the He/CO_2 mixture target: 11 days

- The data will provide 5 to 13% statistical uncertainty

→ The uncertainty of $^{14}O(\alpha,p)^{17}F$ reaction rate: the two orders of magnitude down.

E_x (MeV)	$J^{\pi a}$	Γ_α(keV)[a]	Γ_p(keV)[a]	σ (mb)[b]	Expected counts per bin[c]
6.150	1^-	2.2×10^{-3}	20	0.2397	60
6.286	3^-	3.4×10^{-4}	25	0.07174	18
7.05	4^+	4.8×10^{-2}	53	3.427	920
7.35	1^-	1.7	12	114.6	31,700

Expected total count rate of astrophysically important resonances.

[Readiness]

- ~~TexAT transportation from US to Japan: TexAT was shipped to Canada in 2019. No issue.~~
- ~~A test with the He/CO_2 mixture gas: 96/4% ratio was tested. No issue expected with 90/10% ratio.~~
- ~~Maximum beam rate of the TexAT: The rate 3x10^5 pps in the CD_4 gas was successfully tested when we stopped the beam in the active area~~: 5x10^5 pps tested last August.
- Installation of additional Si detectors on the side and bottom of the active area: Si det. will arrive next week! New frames designs are almost completed.

➔ We are waiting for the beam time after March, 2022!

AToM-X: CENS Active Target TPC

- AToM-X : Active target TPC for Multiple nuclear eXperiment

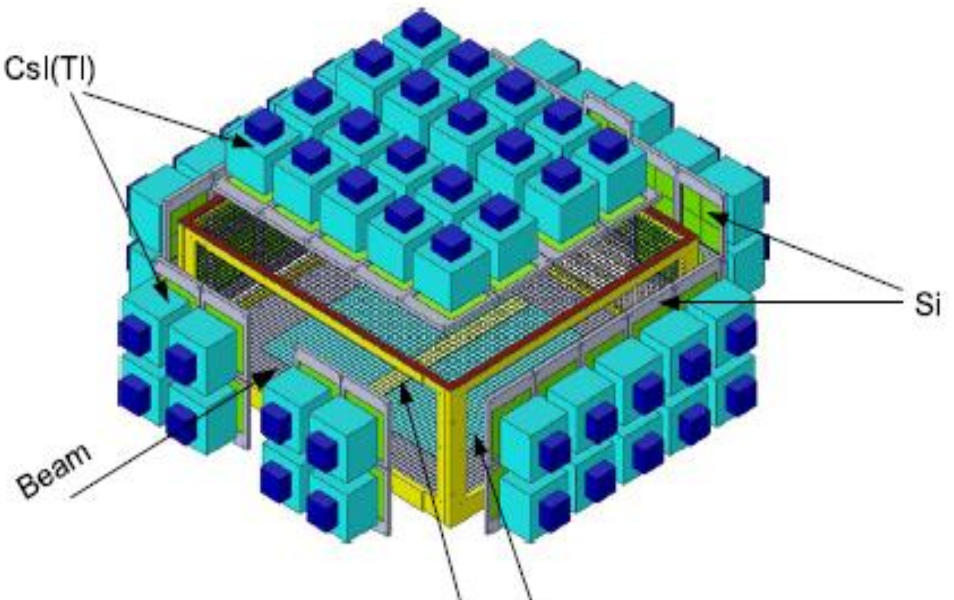

E. Koshchiy et al., NIM A (2020)

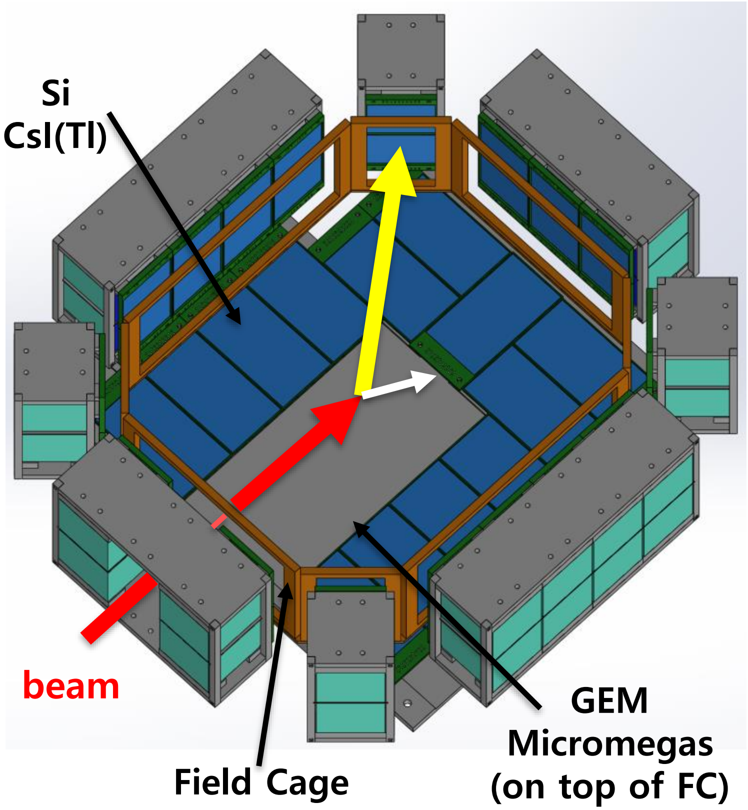

TexAT : Rectangular shape

AToM-X : Octagonal shape

→ No Si dead layer effect!

AToM-X: Silicon and CsI detectors

- Newly designed silicon detector : X6

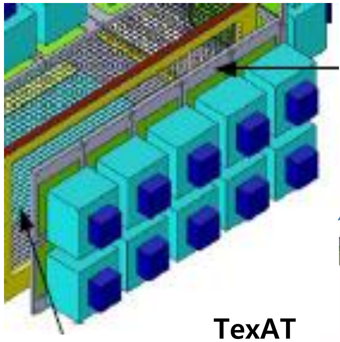

TexAT
(Texas A&M)

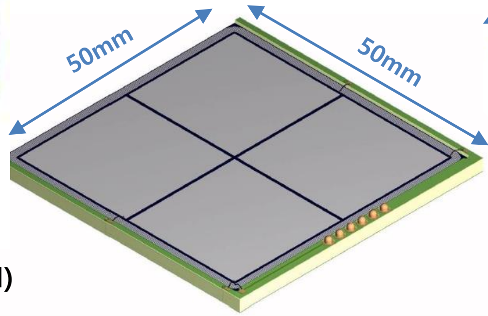

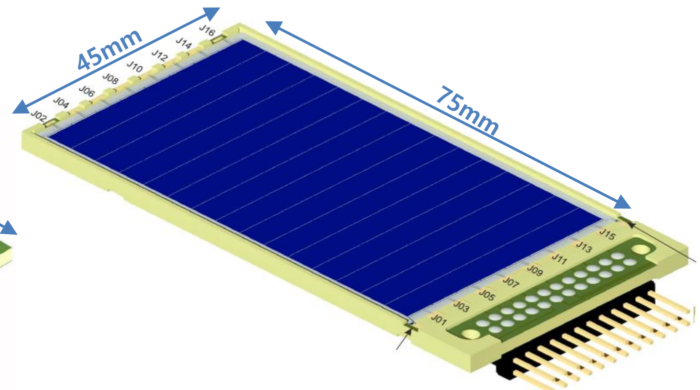

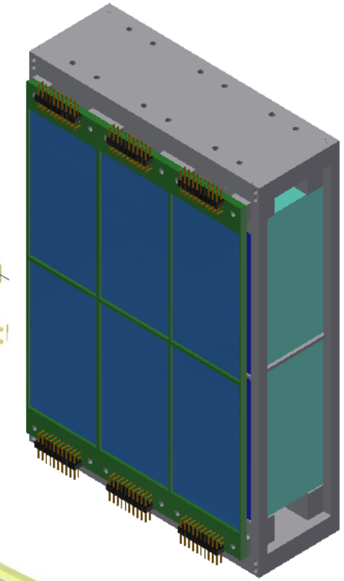

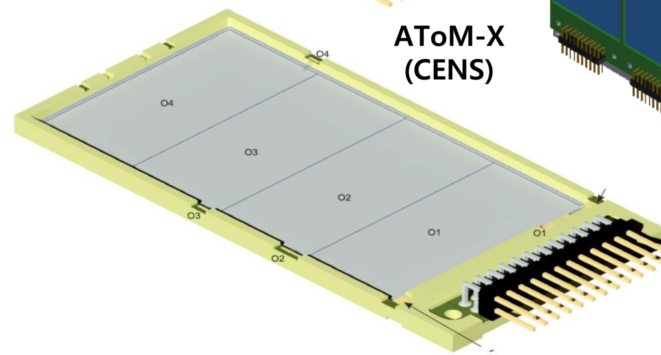

AToM-X
(CENS)

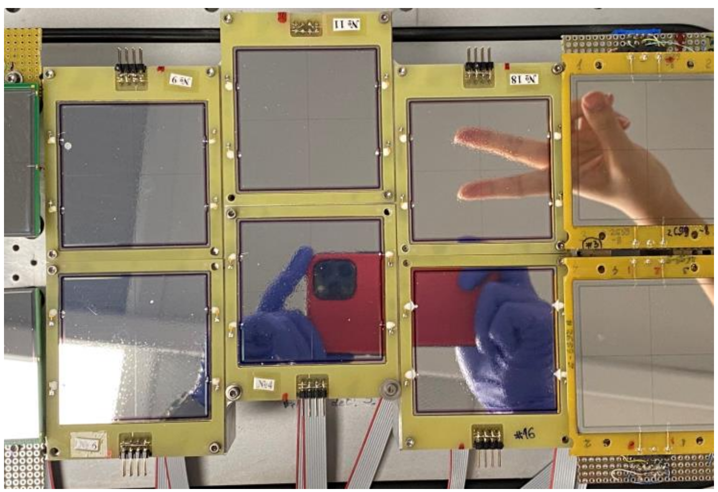

- 8 resistive strips + 4 non-resistive strips

→ Position resolution improved !

- Now waiting for the delivery

AToM-X: DAQ & Analysis software

- Large number of channels (~5000ch)
  - → ASIC Electronics : low cost, small space, and simple setup
  - → GET (Generic Electronics for TPC) : 64ch/chip, 256ch/AsAd board
- DAQ libraries were installed !
- GEANT4-based simulation software
- Track reconstruction/analysis software using machine learning

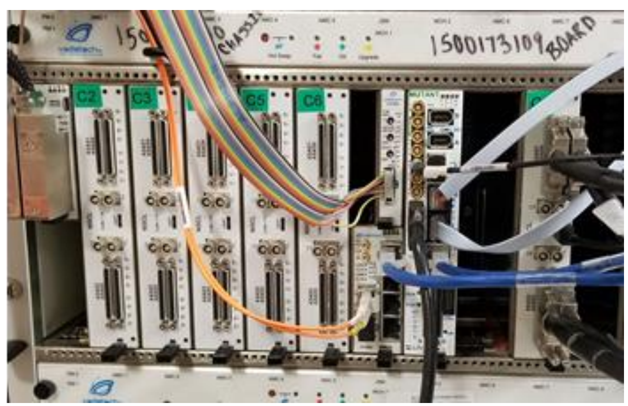

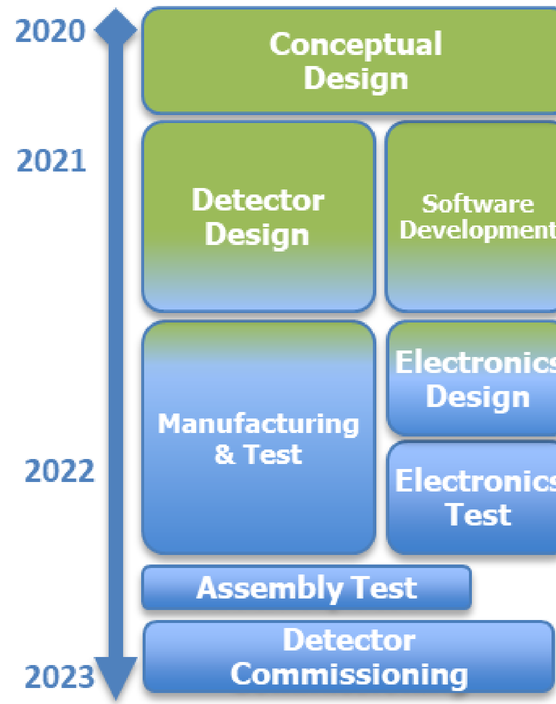

AToM-X: Plan for the future experiment

Direct measurements

of the astrophysically-important (α,p) reactions

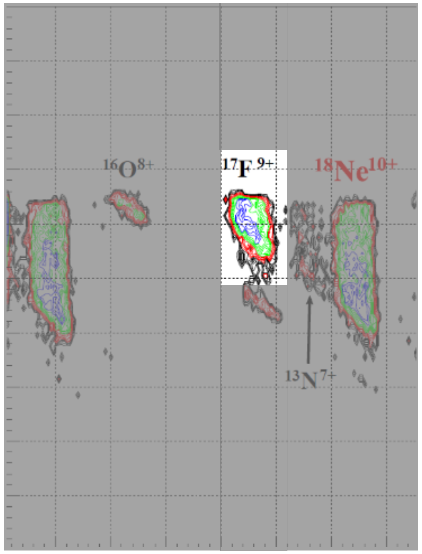

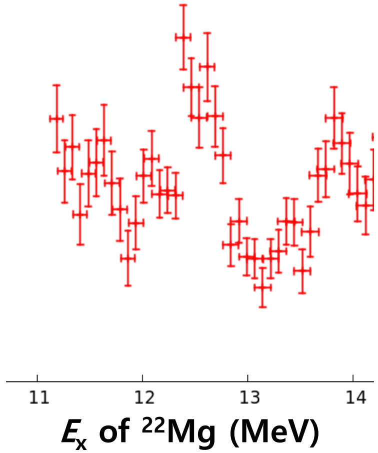

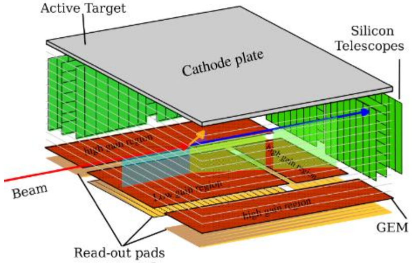

Reactions that Impact the Burst Light Curve in the Single-zone X-Ray Burst Model

Rank	Reaction	Type[a]	Sensitivity[b]	Category
1	^{56}Ni(α, p)^{59}Cu	U	12.5	1
2	^{59}Cu(p, γ)^{60}Zn	D	12.1	1
3	^{15}O(α, γ)^{19}Ne	D	7.9	1
4	^{30}S(α, p)^{33}Cl	U	7.8	1
5	^{26}Si(α, p)^{29}P	U	5.3	1
6	^{61}Ga(p, γ)^{62}Ge	D	5.0	1
7	^{23}Al(p, γ)^{24}Si	U	4.8	1
8	^{27}P(p, γ)^{28}S	D	4.4	1
9	^{63}Ga(p, γ)^{64}Ge	D	3.8	1
10	^{60}Zn(α, p)^{63}Ga	U	3.6	1
11	^{22}Mg(α, p)^{25}Al	D	3.5	1
12	^{56}Ni(p, γ)^{57}Cu	D	3.4	1
13	^{29}S(α, p)^{32}Cl	U	2.8	1
14	^{28}S(α, p)^{31}Cl	U	2.7	1
15	^{31}Cl(p, γ)^{32}Ar	U	2.7	1
16	^{35}K(p, γ)^{36}Ca	U	2.5	2
17	^{18}Ne(α, p)^{21}Na	D	2.3	2
18	^{25}Si(α, p)^{28}P	U	1.9	2
19	^{57}Cu(p, γ)^{58}Zn	D	1.7	2
20	^{34}Ar(α, p)^{37}K	U	1.6	3
21	^{24}Si(α, p)^{27}P	U	1.4	3
22	^{22}Mg(p, γ)^{23}Al	D	1.1	3
23	^{65}As(p, γ)^{66}Se	U	1.0	3
24	^{14}O(α, p)^{17}F	U	1.0	3
25	^{40}Sc(p, γ)^{41}Ti	D	0.9	3
26	^{34}Ar(p, γ)^{35}K	D	0.8	3
27	^{47}Mn(p, γ)^{48}Fe	D	0.8	3
28	^{39}Ca(p, γ)^{40}Sc	D	0.8	3

R.H. Cyburt *et al.*, PRC (2016)

^{17}F(α,p)^{20}Ne

^{18}Ne(α,p)^{21}Na

^{22}Mg(α,p)^{25}Al
^{30}S(α,p)^{33}Cl

and so on…

Optical Model Potentials for Exotic Nuclei

- Can we trust the Global Optical Model Potentials?
  - Phenomenological GOMP
  - Microscopic GOMP

✓ Broad range of lab energy usingAToM-X.

✓ Using ^{16,18}O, ^{20,22}Ne beams, (p,p), (d,d),(α,α) elastic scatterings will be measured.

Optical model potential from chiral effective field theory

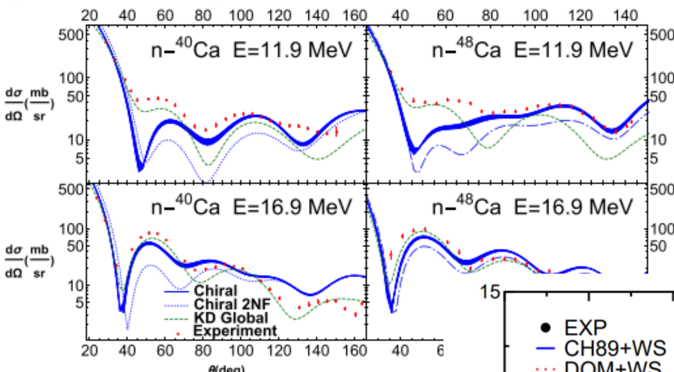

T.R. Whitehead *et al.* PRC (2020)

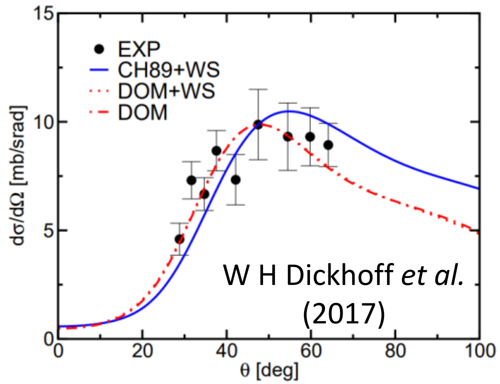

Angular distributions for ^{132}Sn(d,p)^{133}Sn (Ed = 9.46 MeV)

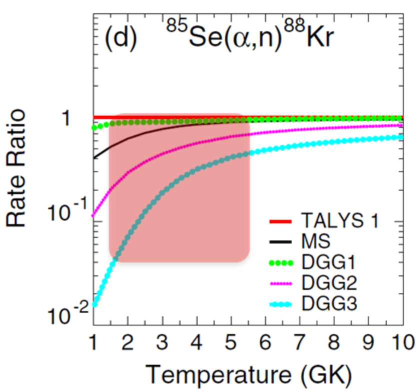

Uncertainty of ^{85}Se(α,n) reaction rate

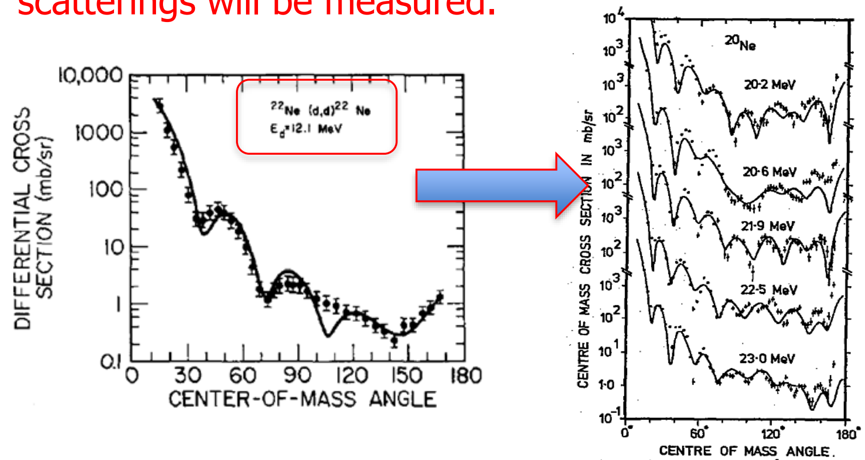

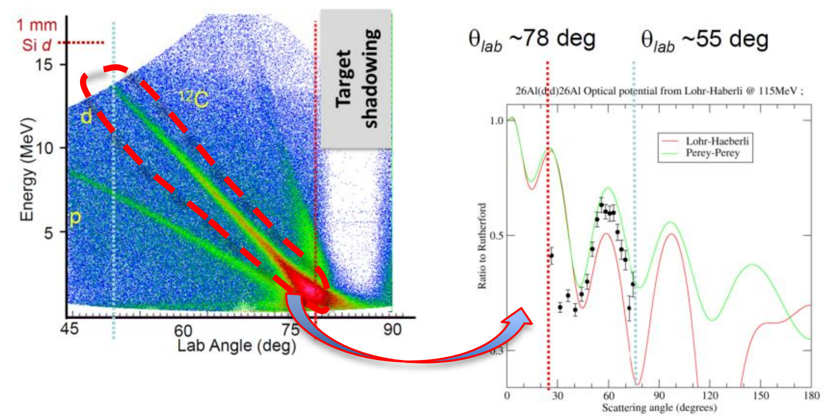

Fusion Reaction Mechanism related to Stellar Evolution

J.C. Zamora *et al.*, PLB (2020)

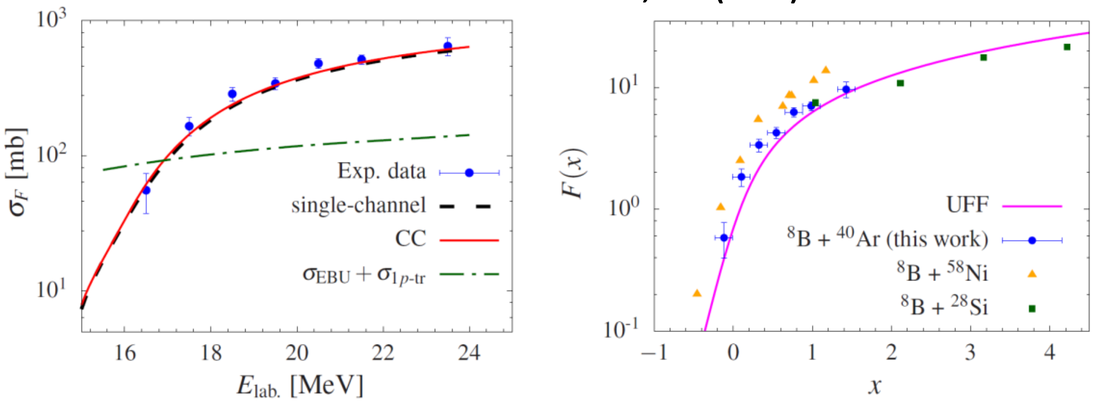

Total fusion excitation function for $^8B + ^{40}Ar$.

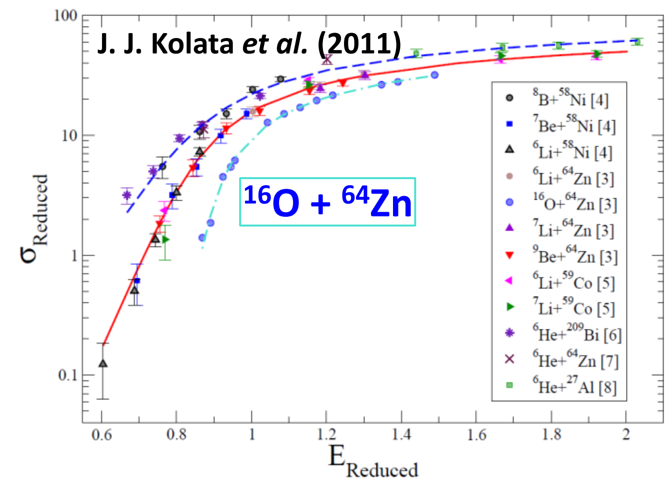

Reduced total reaction cross sections

^{16}O + ^{40}Ar fusion cross sections??

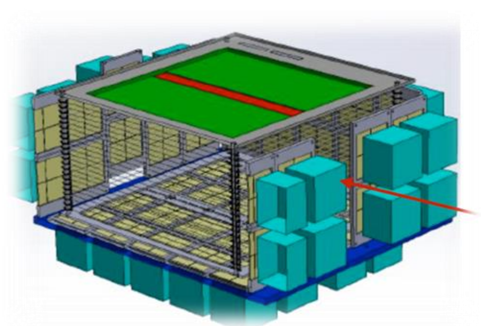

Texas Active Target (TexAT) design

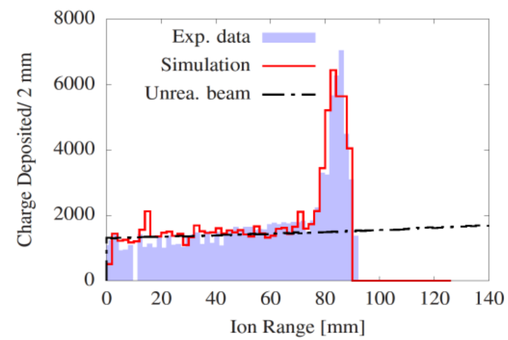

Ionization beam profile for a typical fusion event

- ✓ $^{20}Ne+^{20}Ne$, $^{20}Ne+^{16}O$ fusion cross sections to revisit the result of D. Shapira PRC (1983)
- ✓ Fusion cross sections with halo nucleus (^6He, ^7Li, ^7Be, ^9Be)

Targets and Detectors for Nuclear Astrophysics Studies at CENS

- ✓ Solid Targets: CH_2, CD_2
- ✓ Gas Targets: H_2, D_2, ^4He, ^3He, N_2

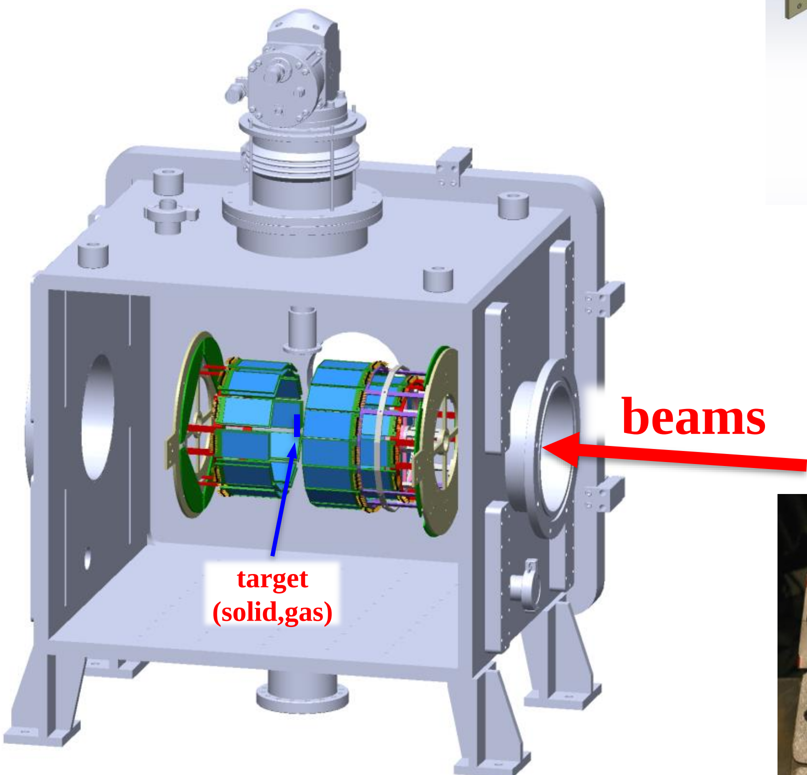

Conceptual Design of STARK chamber

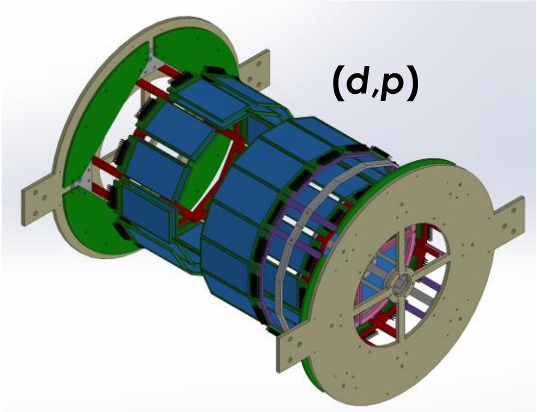

Conceptual Design of STARK

Year 2022!!

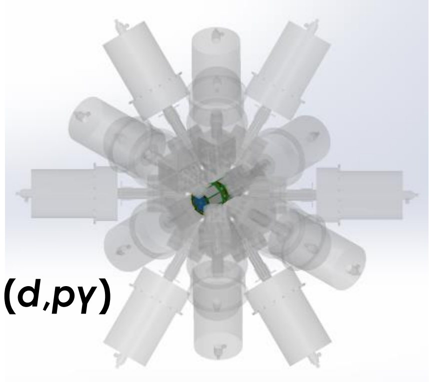

Conceptual Design of STARK Jr. and ASGARD

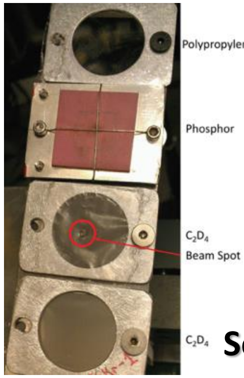

Solid Targets

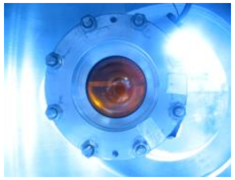

Gas Cell Target

Portable HPGe detectors

Sunghoon(Tony) Ahn

Summary

- Many astrophysical observables can be explained by various nuclosynthesis models.
- Nuclear Physics inputs play an important role in nucleosynthesis calculation results.
- Recent sensitivity studies show large uncertainties on the nuclear properties of unstable nuclei.

➔ **Experimental measurements with rare isotopes are very critical to reduce them.**

- The $^{14}O(\alpha,p)^{17}F$ reaction is one of the most important reactions in the X-ray burst model and a key reaction determining alternate break-out path from HCNO cycle.
- Previous indirect measurements show large disagreements.

➔ **Direct measurement of $^{14}O(\alpha,p)^{17}F$ cross sections using the TexAT will be performed at CRIB/RIKEN, Japan.**

- CENS AT-TPC, AToM-X, is under development for direct measurements of many astrophysically-important (α,p) reactions, elastic scatterings and fusion cross sections.

➔ **$^{17}F(\alpha,p)^{20}Ne$, $^{18}Ne(\alpha,p)^{21}Na$, $^{22}Mg(\alpha,p)^{25}Al$, $^{30}S(\alpha,p)^{33}Cl$ and more…**

Thank you!

CENS, IBS:
K. I. Hahn, S. Ahn, D. Kim, J.W. Hwang, B. Moon, C.Y. Park, S.H. Bae, and S.M. Cha

Sungkyunkwan Univ.:
K.Y. Chae, M.J. Kim, C.H. Kim, and S.H. Kim

Texas A&M Univ.:
G. V. Rogachev, E. Koshchiy, J. Bishop, and C. Parker

CEA, Saclay, France:
L. Pollacco

and YOU in the future!